DALTON

Redox behaviour of 4Fe-4S ferredoxin model arenethiolate complexes involving specific NH · · · S hydrogen bonds assisted by a neighbouring phenyl group

Takafumi Ueno, Norikazu Ueyama and Akira Nakamura *

Department of Macromolecular Science, Faculty of Science, Osaka University, Toyonaka, Osaka 560, Japan

The complexes $[NMe_4]_2[Fe_4S_4(SC_6H_3Ph\text{-}6\text{-}NHCOR'\text{-}2)_4]^{2-}$ (R' = Bu^t **1**, Me **2** or CF_3 **3**), $[NMe_4]_2[Fe_4S_4(SC_6H_3Ph\text{-}6\text{-}NHCOR'\text{-}4)_4]^{2-}$ (R' = Bu^t **4** or CF_3 **5**) and $[NMe_4]_2[Fe_4S_4(SC_6H_3Et\text{-}6\text{-}NHCOBu^t\text{-}2)_4]^{2-}$ **6** were synthesized by ligand-exchange reactions of $[NMe_4]_2[Fe_4S_4(SBu^t)_4]^{2-}$ with the corresponding organic disulfides. They have been characterized by IR and UV/VIS spectroscopy and by elemental microanalyses. From IR spectra in the solid state, the ν(NH) shift (114 cm^{-1}) of **1** from the band of the corresponding disulfide is larger than that of **6** (87 cm^{-1}). The results indicate that the phenyl group at the 6 position contributes to the strengthening of the NH · · · S hydrogen bond. The stabilization of the $[Fe_4S_4(SR)_4]^{-}$–$[Fe_4S_4(SR)_4]^{2-}$ redox potential of **1** compared with **6** is due to the co-operation of the aromatic ring and this hydrogen bond.

Iron–sulfur proteins are important electron-transfer proteins. For example, high-potential iron–sulfur proteins (HiPIPs) and ferredoxins (Fds) have a [4Fe-4S] cluster co-ordinated with four cysteinyl sulfur ligands at their active sites. Upon electron transfer, HiPIPs use the $[Fe_4S_4(SR)_4]^{2-}$–$[Fe_4S_4(SR)_4]^{-}$ redox reaction. On the other hand, Fds utilize the $[Fe_4S_4(SR)_4]^{3-}$–$[Fe_4S_4(SR)_4]^{2-}$ redox reaction. The relation between the environment of a [4Fe-4S] cluster and the redox behaviour still remains unclear. Crystal structure analysis of HiPIPs indicates that the four aromatic rings and the five NH · · · S hydrogen bonds have been preserved at the active site [Fig. 1(*a*)].[1,2] The amino acid sequence of Fds indicates that two aromatic rings and eight NH · · · S hydrogen bonds have been preserved,[3] but the effects of the aromatic ring and the NH · · · S hydrogen bond are still unknown.

The [4Fe-4S] clusters with bulky ligands such as 2,4,6-triisopropylbenzenethiolate,[4] tripeptide,[4] 36-membered macrocyclic thiolates[5] and adamantane-1-thiolate[6] exhibit quasi-reversible $[Fe_4S_4(SR)_4]^{2-/-}$ redox couples in organic solvents or aqueous solutions. However, other factors are thought to stabilize the redox couple and to modulate the redox potential because native HiPIPs undergo a reversible one-electron-transfer reaction at a characteristically high oxidation–reduction midpoint potential in the range of −0.19 to +0.21 V *vs.* saturated calomel electrode (SCE).[7] For example, an interaction between aromatic residues and sulfur atoms has been proposed from a ^{1}H NMR investigation of *Ectothiorhodospira halophila* and *Ectothiorhodospira vacuolata* HiPIPs.[8] In addition, the direct interaction of an aromatic ring with the Fe–S cluster in *Chromatium vinosum* HiPIP has been demonstrated by ^{19}F NMR spectroscopy.[9]

The above results imply that the chemical environments of the ligating cysteine sulfur atoms are important because non-covalent interactions between the cysteinate ligand and the nearby amino acids can have an influence on the electron-transfer reaction. We have verified the chemical role of the NH · · · S hydrogen bond on the redox potential using ferredoxin model complexes with peptide ligands[10,11] or various simple 2-mono- and 2,6-di-acylaminobenzenethiolate ligands.[12] The NH · · · S hydrogen bond contributes not only to a positive shift of the redox potential but also to the prevention of [4Fe-4S] core extrusion with benzenethiolate.[12]

In this paper we report a study of the effect of the neighbouring aromatic rings and NH · · · S hydrogen bonds on the function of [4Fe-4S] clusters by using the novel thiolate ligands, 2-R'CONH-6-$PhC_6H_3S^-$ [Fig. 1(*b*)] and 2-R'CONH-6-$EtC_6H_3S^-$ [Fig. 1(*c*)]. An advantage of these ligands is their ability to bring about reproducible hydrophobic environments which enforces the NH · · · S hydrogen bonds just as is observed in native HiPIPs and Fds.

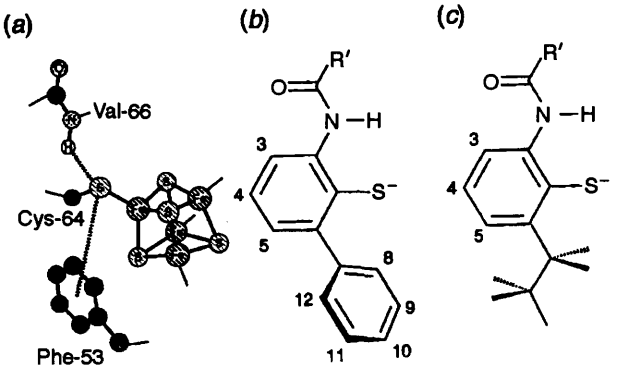

Fig. 1 Schematic drawings of (*a*) the non-covalent interaction of *E. halophila* HiPIP, (*b*) 2-R'CONH-6-$PhC_6H_3S^-$ and (*c*) 2-R'CONH-6-$EtC_6H_3S^-$

Results and Discussion

Infrared spectra of $[Fe_4S_4(SR)_4]^{2-}$ and the corresponding organic disulfides

In order to detect the presence of the NH · · · S hydrogen bond the IR spectra of the complexes were measured in the solid state. Table 1 shows selected IR bands of $[Fe_4S_4(SR)_4]^{2-}$ and the differences from the corresponding organic disulfide. Fig. 2 shows the amide NH regions in the IR spectra of (*a*) (2-Bu^{t}CONH-6-$PhC_6H_3S)_2$ and (*b*) $[NMe_4]_2[Fe_4S_4(SC_6H_3Ph\text{-}6\text{-}NHCOBu^t\text{-}2)_4]$ **1** in the solid state. Complex **1** exhibits a NH band at 3298 cm^{-1} and a C=O band at 1663 cm^{-1}. The differences, Δν(NH) and Δν(C=O), between **1** and the corresponding disulfide can be estimated at 114 and 27 cm^{-1}, respectively, when the stretching vibration of the corresponding disulfide is employed as a standard. The complex

Table 1 Selected IR bands of $[Fe_4S_4(SR)_4]^{2-}$ and the corresponding disulfide R_2S_2 in the solid state

R	$\tilde{\nu}$(NH)/cm^{-1}	Δν(NH)[a]	$\tilde{\nu}$(C=O)/cm^{-1}	Δν(C=O)[a]
2-Bu^{t}CONH-6-PhC$_6$H$_3$	3298 (3412)[b]	114	1663 (1690)[b]	27
2-MeCONH-6-PhC$_6$H$_3$	3301 (3261)	−40	1683 (1665)	−18
2-CF$_3$CONH-6-PhC$_6$H$_3$	3231 (3375)	144	1710 (1740)	30
4-Bu^{t}CONH-6-PhC$_6$H$_3$	3329 (3324)	−5	1661 (1656)	−5
2-Bu^{t}CONH-6-EtC$_6$H$_3$	3300 (3387)	87	1665 (1691)	26
2-Bu^{t}CONHC$_6$H$_4$[c]	3314 (3389)	75	1670 (1679)	9

[a] Δν = ν(disulfide) − ν(Fe$_4$S$_4$ complex). [b] The value of the corresponding disulfide. [c] Ref. 12.

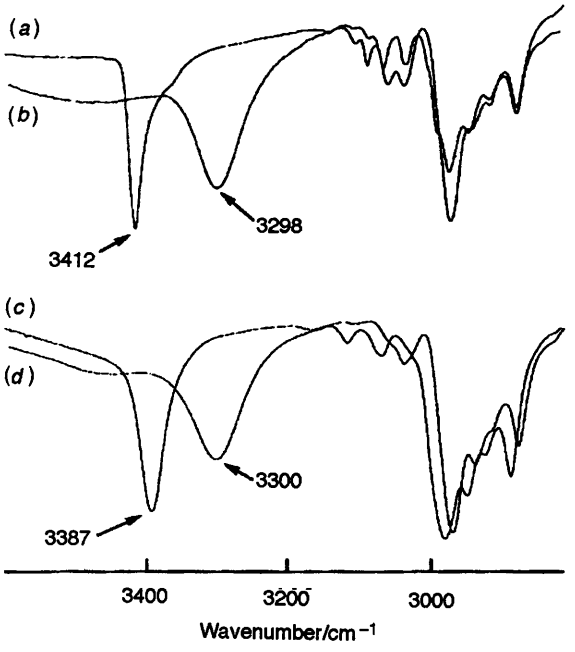

Fig. 2 The ν(NH) region in the IR spectra of (*a*) (2-Bu^{t}CONH-6-PhC$_6$H$_3$S)$_2$, (*b*) $[NMe_4]_2[Fe_4S_4(SC_6H_3Ph\text{-}6\text{-}NHCOBu^t\text{-}2)_4]$ **1**, (*c*) (2-Bu^{t}CONH-6-EtC$_6$H$_3$S)$_2$ and (*d*) $[NMe_4]_2[Fe_4S_4(SC_6H_3Et\text{-}6\text{-}NHCOBu^t\text{-}2)_4]$ **6** in the solid state

$[NMe_4]_2[Fe_4S_4(SC_6H_3Ph\text{-}6\text{-}NHCOBu^t\text{-}4)_4]$ **4** has Δν(NH) of −5 cm^{-1} and Δν(C=O) of −5 cm^{-1}. Similar Δν(NH) values have been observed for various single NH···S hydrogen-bonded metal complexes, *e.g.* 75 cm^{-1} for $[Fe_4S_4(SC_6H_4NHCOBu^t\text{-}2)_4]^{2-}$ (ref. 12) and 59 cm^{-1} for $[Mo^{IV}O(SC_6H_4NHCOBu^t\text{-}2)_4]^{2-}$.[13] These results indicate the presence of a NH···S hydrogen bond in **1** and its absence in **4**. The disulfide (2-MeCONH-6-PhC$_6$H$_3$S)$_2$ shows ν(NH) at 3261 cm^{-1} and ν(C=O) at 1665 cm^{-1} (Table 1) due to NH···O=C hydrogen bonding as observed in (2-Bu^{t}CONHC$_6$H$_4$S)$_2$.[14] Complex **2** shows Δν(NH) of −40 cm^{-1} and Δν(C=O) of −18 cm^{-1} (Table 1) but there is no evidence of NH···S hydrogen-bond formation in the solid state. The NH and C=O bands of $[NMe_4]_2[Fe_4S_4(SC_6H_3Ph\text{-}6\text{-}NHCOCF_3\text{-}2)_4]$ **3** are observed at 3231 and 1710 cm^{-1}, respectively. This complex has NH···S hydrogen bonds because Δν(NH) and Δν(C=O) are 144 and 30 cm^{-1}, respectively. The large Δν(NH) indicates that the strength of the hydrogen bond is similar to that in $[Cu^I(SC_6H_4NHCOMe\text{-}2)_3]^{2-}$ [Δν(NH) 163 cm^{-1}].[15]

Fig. 2(*c*) and (*d*) show the amide NH and C=O regions in the IR spectra of the corresponding disulfide $[NMe_4]_2[Fe_4S_4(SC_6H_3Et\text{-}6\text{-}NHCOBu^t\text{-}2)_4]$ **6** in the solid state. The complex exhibits ν(NH) at 3300 cm^{-1}. Since the differences, Δν(NH) and Δν(C=O), can be estimated to be 87 and 26 cm^{-1} (Table 1), respectively, there is a NH···S hydrogen bond.

In a hydrogen-bonded amide the decrease, Δν(NH), in the frequency of ν(NH) relative to that of the unassociated form is expected to reflect the strength of the hydrogen bond. The Δν(NH) of complexes **1** (114) and **6** (87 cm^{-1}) are larger than the 75 cm^{-1} of $[NEt_4]_2[Fe_4S_4(SC_6H_4NHCOBu^t\text{-}2)_4]$ which is taken as a standard containing a single NH···S hydrogen bond.[12] These results indicate that the hydrogen bonds in **1** and **6** are stronger than those in the standard. In addition, the difference in Δν(NH) between **1** and **6** is 27 cm^{-1}. Thus, the contribution of the phenyl group at the 6 position of **1** to the strengthening of the hydrogen bond is larger than that of the ethyl group at the same position in **6**.

^{1}H NMR spectra

Table 2 shows the ^{1}H NMR chemical shifts of the model complexes in CD$_3$CN at 30 °C. The peaks were assigned by two-dimensional correlation (COSY) and nuclear Overhauser effect spectroscopy (NOESY) methods. Complexes **1** and **4** give NH signals at δ 9.17 and 8.23, respectively. That of **1** is observed at lower field because the NH···S hydrogen bond is formed in **1** as confirmed by IR spectroscopy. The NH signals assignable to the NH···S hydrogen bond of *C. vinosum* HiPIP$_{red}$ have been observed in a similar region (δ 8.39–7.53) in aqueous solution.[16] The peaks due to the hydrogen at position 6 of the phenyl groups in **1**–**5** are observed at similar positions. The T_1 value of H^{8,12} in **1** is 12 ms. Signals due to aromatic rings close to the [4Fe-4S] cluster of *C. vinosum* HiPIP$_{red}$ have also been observed in the typical aromatic region.[16] The T_1 value of the aromatic ring of Phe adjacent to the [4Fe-4S] cluster of *C. vinosum* HiPIP$_{red}$ is 11 ms.[17] These results indicate that in CD$_3$CN complex **1** has a NH···S hydrogen bond and a phenyl ring close to the [4Fe-4S] cluster.

Table 3 summarizes the isotropic shifts for these complexes. The isotropic shift of protons H$^{2-5}$ is essentially similar to those of ferredoxin model complexes with *p*-substituted benzenethiolate complexes which have been studied in detail.[18] The isotropic shift of the NH···S hydrogen-bonded NH signal for **6** is 0.15 ppm. Slight isotropic shifts have been observed for $[Fe_4S_4\{SC_6H_3(NHCOBu^t)\text{-}2,6\}_4]^{2-}$ (ref. 12) and various [4Fe-4S] peptide model complexes.[11] On the other hand, the isotropic shifts of the NH signal for **1**–**3** are larger, 0.78, 1.24 and 1.51 ppm, respectively. In addition, those of the H^{8,12} signal for **1**–**3** are 0.87, 0.80 and 0.77 ppm, respectively, larger than those of **4** (0.43) and **5** (0.39 ppm). The chemical shifts of the ring protons of $[Fe_4S_4\{C_6H_4(SCH_2)_2\text{-}1,3\}_2]^{2-}$ can be perturbed as a consequence of a roughly parallel orientation of the phenyl ring with respect to the cluster.[18] The results suggest that the co-existence of the NH···S hydrogen bond and the phenyl ring contributes to the perturbation of the isotropic shifts for the NH and H^{8,12} signals.

UV/VIS spectra

The solution spectra were recorded in the 250–700 nm region, which corresponds to that commonly measured for Fd$_{ox}$ and HiPIP$_{red}$ proteins. Fig. 3 shows the electronic spectra of complexes **1**, **4** and **6** in acetonitrile at room temperature and Table 4 gives the absorption maxima of the complexes in acetonitrile at room temperature.

The results indicate a different type of absorption maximum

Table 2 Chemical shift data * for $[Fe_4S_4(SR)_4]^{2-}$ in CD_3CN at 30 °C

	δ								
R	H^2	H^3	H^4	H^5	NH	$H^{8,12}$	H^{9-11}	Others	NMe_4^+
2-Bu^{t}CONH-6-PhC_6H_3	—	9.56	6.30	7.84	9.17	7.57	7.24	1.25 (Bu^t)	3.03
2-MeCONH-6-PhC_6H_3	—	9.42	6.32	7.97	9.36	7.59	7.30	2.23 (CH_3)	3.01
2-CF_3CONH-6-PhC_6H_3	—	9.35	6.36	8.01	10.23	7.58	7.23	—	3.03
4-Bu^{t}CONH-6-PhC_6H_3	7.25	8.67	—	8.47	8.23	7.67	7.38	1.25 (Bu^t)	2.98
4-CF_3CONH-6-PhC_6H_3	7.29	8.67	—	8.50	9.52	7.66	7.43	—	3.01
2-Bu^{t}CONH-6-EtC_6H_3	—	9.34	6.10	7.96	8.75		—	3.73 (CH_2CH_3), 1.52 (CH_2CH_3), 1.31 (Bu^t)	3.04

* In ppm from $SiMe_4$.

Table 3 Hydrogen-1 isotropic shifts of $[Fe_4S_4(SR)_4]^{2-}$ in CD_3CN at 30 °C

	Isotropic shift/ppm							
R	H^2	H^3	H^4	H^5	NH	$H^{8,12}$	H^{9-11}	Others
2-Bu^{t}CONH-6-PhC_6H_3	—	1.28	−1.08	0.97	0.78	0.87	0.03	0.04 (Bu^t)
2-MeCONH-6-PhC_6H_3	—	1.30	−1.06	1.06	1.24	0.80	0.06	0.31 (CH_3)
2-CF_3CONH-6-PhC_6H_3	—	1.37	−1.11	0.92	1.51	0.77	−0.03	
4-Bu^{t}CONH-6-PhC_6H_3	−0.21	1.10	—	1.00	0.22	0.43	−0.01	0.01 (Bu^t)
4-CF_3CONH-6-PhC_6H_3	−0.17	1.14	—	0.98	0.29	0.39	0.04	
2-Bu^{t}CONH-6-EtC_6H_3	—	1.17	−1.24	0.94	0.15	—	—	0.46 (CH_2CH_3), 1.12 (CH_2CH_3), 0.19 (Bu^t)

* Isotropic shift = $(\Delta H/H_0)_{obs} - (\Delta H/H_0)_{dia}$: where the diamagnetic references are for the corresponding disulfides in CD_3CN at 30 °C.[18]

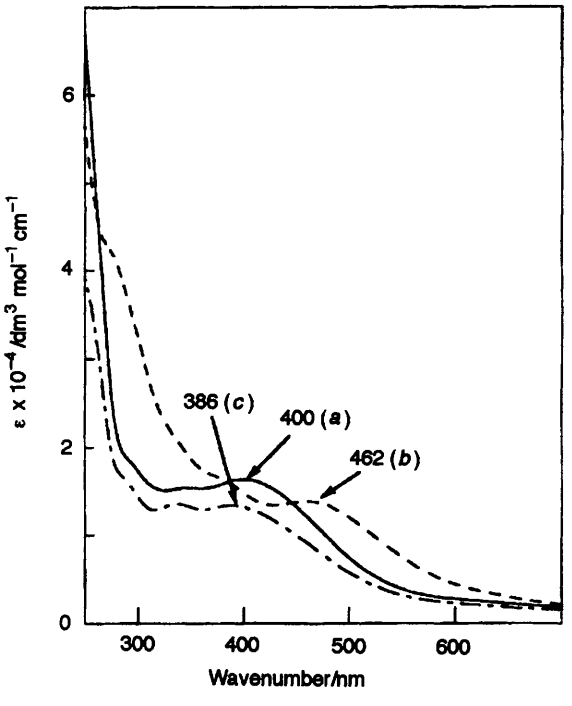

Fig. 3 The UV/VIS spectra of (*a*) $[Fe_4S_4(SC_6H_3Ph\text{-}6\text{-}NHCOBu^t\text{-}2)_4]^{2-}$ **1**, (*b*) $[Fe_4S_4(SC_6H_3Ph\text{-}6\text{-}NHCOBu^t\text{-}4)_4]^{2-}$ **4** and (*c*) $[Fe_4S_4(C_6H_3Et\text{-}6\text{-}NHCOBu^t\text{-}2)_4]^{2-}$ **6** in acetonitrile at room temperature

for the 2,6-substituted complexes (**1–3** and **6**) compared to the 2,4-substituted complexes (**4** and **5**). The same trend has been reported for methyl-substituted arenethiolate complexes. Actually, $[Fe_4S_4(SC_6H_2Me_3\text{-}2,4,6)_4]^{2-}$ (ref. 4) and $[Fe_4S_4(SC_6H_4Me\text{-}2)_4]^{2-}$ (ref. 20) exhibit absorption maxima at 409 (29 200) and 460 nm (18 300 dm^3 mol^{-1} cm^{-1}) in dimethylformamide (dmf), respectively. The prevention of a p_π–p_π conjugation between the sulfur and the benzene ring by steric hindrance with the 2,6-methyl groups results in a different visible absorption maximum when compared to that for

Table 4 The UV/VIS spectral data for $[Fe_4S_4(SR)_4]^{2-}$ in acetonitrile at room temperature

R	λ_{max}/nm (ε/dm^3 mol^{-1} cm^{-1})
2-Bu^{t}CONH-6-PhC_6H_3	400 (16 400)
2-MeCONH-6-PhC_6H_3	400 (17 100)
2-CF_3CONH-6-PhC_6H_3	385 (16 000)
4-Bu^{t}CONH-6-PhC_6H_3	462 (13 900)
4-CF_3CONH-6-PhC_6H_3	453 (15 600)
2-Bu^{t}CONH-6-EtC_6H_3	338 (13 600), 386 (13 400)
C. vinosum $HiPIP_{red}$ in water	388 (16 000) *

* Ref. 19.

$[Fe_4S_4(SC_6H_4Me\text{-}2)_4]^{2-}$.[20] Thus, the 2-acylamino, 6-phenyl and -ethyl groups of **1–3** and **6** seem to prevent p_π–p_π conjugation between the sulfur and the benzene ring. More detailed structural parameters are required for a discussion of the π conjugation, but attempts to analyse the crystal structures of these complexes were unsuccessful.

The absorption maxima of complexes **1–3** and **6** are similar to those of $HiPIPs_{red}$ and Fds_{ox}. Native cysteine-containing Fds_{ox} and $HiPIPs_{red}$ in aqueous solution have been reported to exhibit maxima at 385–400 nm, *e.g.* 390 nm for *B. stearothermophilus* Fd_{ox} and 388 nm for *C. vinosum* $HiPIP_{red}$.[19] The absorption maxima in this region have been theoretically proposed to be due to ligand S→Fe charge transfer.[21] For complexes **1–3** and **6** the prevention of the p_π–p_π conjugation results in a similar Fe–S interaction to that of an alkanethiolate ligand like that of cysteine. Alkanethiolate model complexes have shown absorption maxima at 400–420 nm. For example, $[NEt_4]_2[Fe_4S_4(SCH_2Ph)_4]$ exhibits maximum at 420 nm (18 500 dm^3 mol^{-1} cm^{-1}) in dmf at room temperature.[22] Furthermore, **1–3** and **6** show blue-shifted visible absorption maxima when compared to the alkanethiolate complexes because the NH···S hydrogen bond interacts with the sulfur p_π orbital and decreases the occupied MO energy levels.[12] In the present model complexes the phenyl or ethyl groups at the 6 position construct a hydrophobic layer around the [4Fe-4S] cluster. The presence of aromatic rings, alkyl chains and a NH···S

hydrogen bond near the cysteinyl sulfur atoms has been confirmed in the [4Fe-4S] core environments of Fds and HiPIPs by X-ray crystallographic analyses.[3]

The similarity between the absorption maxima observed for Fds and HiPIPs in water and those of the model complexes in the less-polar acetonitrile suggests that a co-operative effect between the NH···S hydrogen bond and the hydrophobic groups contributes to the control of S→Fe charge transfer in $HiPIPs_{red}$ and also in Fds_{ox}.

Electrochemical properties

The model complexes exhibit two quasi-reversible redox couples of $[Fe_4S_4(SR)_4]^{-}$–$[Fe_4S_4(SR)_4]^{2-}$ and $[Fe_4S_4(SR)_4]^{2-}$–$[Fe_4S_4(SR)_4]^{3-}$ in acetonitrile at room temperature. Fig. 4 shows the cyclic voltammograms of **1** and **6** in acetonitrile at room temperature; the corresponding data are given in Table 5. The contribution of the NH···S hydrogen bond to the positive shift (*ca.* 0.2 V) of redox potential in the synthetic analogues is larger than that of native proteins (from 0.072 to 0.076 V).[24] Complex **1** gives a quasi-reversible 1−/2− redox couple at +0.16 V *vs.* SCE ($i_{p,c}/i_{p,a}$ = 0.76), while the 2−/3− redox couple is observed at −1.05 V ($i_{p,c}/i_{p,a}$ = 0.31) with poor reversibility. Complex **6** exhibits a 1−/2− redox couple at +0.23 V ($i_{p,c}/i_{p,a}$ = 0.62) and a 2−/3− couple at −1.02 V ($i_{p,c}/i_{p,a}$ = 0.83). Complex **1** shows a positive shift of 0.15 V from the 2−/3− redox couple of $[Fe_4S_4(SC_6H_2Me_3\text{-}2,4,6)_4]^{2}$ (−1.20 V *vs.* SCE in acetonitrile)[23] and a negative shift of 0.25 V from that of $[Fe_4S_4\{SC_6H_3(NHCOBu^t)_2\text{-}2,6\}_4]^{2-}$ (−0.80 V *vs.* SCE in acetonitrile).[12] Complex **6** shows corresponding shifts of 0.18 and 0.22 V. The results indicate that each hydrogen bond provides a *ca.* 0.2 V positive shift for the couple $[Fe_4S_4(SR)_4]^{3-}$–$[Fe_4S_4(SR)_4]^{2-}$. The shift is attributed only to the electronic effect of the hydrogen bond. The absence of electronic conjugation is evident because there is no p_π–p_π conjugation between the sulfur and the benzene ring as recognized from the UV/VIS spectral data.[12,25]

The 400 mV difference in the redox potentials between *Rhodopseudomonas globiformis* HiPIP (210 mV *vs.* SCE) and *E. halophilia* (190 mV)[7] cannot be explained by the hydrophobic environments alone, but rather by other factors, such as the co-operative effect of the aromatic ring and the NH···S hydrogen bond. There are six aromatic residues surrounding the cluster in *E. halophila* HiPIP and five such residues near the *C. vinosum* HiPIP cluster. However, only four are located in the binding pocket in *Rhodocyclus tenuis* HiPIP.[2] All three of the HiPIPs show very similar hydrogen-bonding patterns to sulfurs at the redox centre.[2] In addition, non-polar side chains surrounding the HiPIP clusters differ considerably from those found in the Fd cluster. Specifically, the HiPIP cavity chiefly contains aromatic amino acid side chains, whereas the Fd active site includes many aliphatic amino acid side chains.[3] Comparing complexes **1** and **6**, the former, has a more stable $[Fe_4S_4(SR)_4]^{2-}$–$[Fe_4S_4(SR)_4]^{-}$ redox couple ($i_{p,c}/i_{p,a}$ = 0.76) than $[Fe_4S_4(SR)_4]^{3-}$–$[Fe_4S_4(SR)_4]^{2-}$ ($i_{p,c}/i_{p,a}$ = 0.31). However, for **6** the $[Fe_4S_4(SR)_4]^{3-}$–$[Fe_4S_4(SR)_4]^{2-}$ couple ($i_{p,c}/i_{p,a}$ = 0.83) is more stable. The electrochemical results show that the co-existence of an aromatic ring and a NH···S hydrogen bond contributes to the stabilization of the $[Fe_4S_4(SR)_4]^{2-}$–$[Fe_4S_4(SR)_4]^{-}$ redox reaction.

Conclusion

In the case of our model complexes, the co-existence of the aromatic ring and the NH···S hydrogen bond contributes to the stabilization of the $[Fe_4S_4(SR)_4]^{2-}$–$[Fe_4S_4(SR)_4]^{-}$ redox reaction by the positive shift of its potential. The IR spectral data (Table 1) indicate that the aromatic ring of **1** strengthens the NH···S hydrogen bond. The isotropic shift data (Table 3) revealed the existence of the interaction between the NH···S hydrogen bond and the phenyl group indirectly. Previous papers have shown that [4Fe-4S] model complexes having a single or double NH···S hydrogen bonds exhibit a positively shifted $[Fe_4S_4(SR)_4]^{3-}$–$[Fe_4S_4(SR)_4]^{2-}$ redox couple and an irreversible $[Fe_4S_4(SR)_4]^{2-}$–$[Fe_4S_4(SR)_4]^{-}$ redox couple in acetonitrile,[12] and the hydrophobic bulky group was found to contribute to stabilization of the latter couple.[4,26]

In the case of native HiPIPs, one of the roles of the aromatic rings is probably to contribute to the strengthening of the NH···S hydrogen bond and the co-operative effect between the aromatic rings and such bonds seems to result in the positive shift in the $[Fe_4S_4(SR)_4]^{2-}$–$[Fe_4S_4(SR)_4]^{-}$ redox potential.

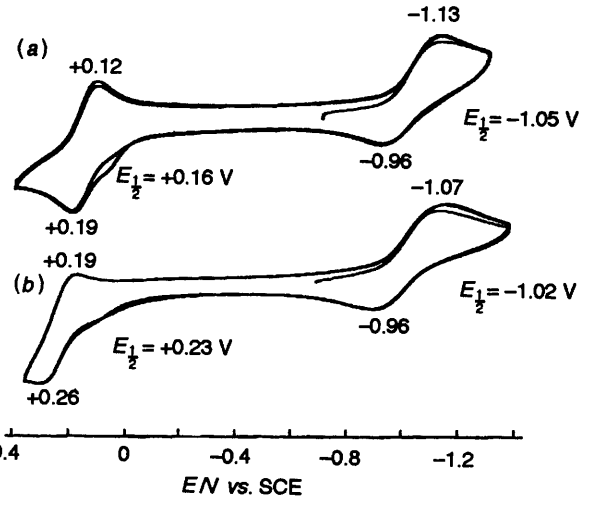

Fig. 4 Cyclic voltammograms of (*a*) complex **1** and (*b*) **6** in acetonitrile at room temperature. Scanning rate 100 mV s^{-1}; complex concentration 2.5 mmol dm^{-3} in the presence of 0.1 mol dm^{-3} $NBu^n_4ClO_4$

Table 5 Redox potentials (*vs.* SCE) of $[Fe_4S_4(SR)_4]^{2-}$ in acetonitrile at room temperature

	1−/2− Couple		2−/3− Couple	
R	$E_{\frac{1}{2}}$/V	i_{pc}/i_{pa}	$E_{\frac{1}{2}}$/V	i_{pa}/i_{pc}
2-Bu^{t}CONH-6-PhC_6H_3	+0.16	0.76	−1.05	0.31
2-MeCONH-6-PhC_6H_3	+0.30	0.14	−0.91	0.82
2-CF_3CONH-6-PhC_6H_3	+0.28	0.56	−0.90	0.68
4-Bu^{t}CONH-6-PhC_6H_3	—		−1.01	1.00
4-CF_3CONH-6-PhC_6H_3	—		−0.93	1.00
2-Bu^{t}CONH-6-EtC_6H_3	+0.23	0.62	−1.02	0.83
2,6-$(Bu^tCONH)_2C_6H_3$[a]	—		−0.80	
2,4,6-$Me_3C_6H_2$[b]	0.00		−1.20	

[a] Ref. 12. [b] Ref. 23.

Experimental

General methods and materials

All procedures were performed in an argon atmosphere by the Schlenk technique. All solvents were dried over calcium hydride and distilled before use. 2-Aminobiphenyl and 2-ethylaniline were obtained from Tokyo Kasei Co. 2-Amino-3-nitrobiphenyl, 2-amino-5-nitrobiphenyl and 2-ethyl-6-nitroaniline were prepared by literature methods.[27,28] 2-Nitro-6-phenylphenyl thiocyanate, 4-nitro-6-phenylphenyl thiocyanate and 2-nitro-6-ethylphenyl thiocyanate were prepared by modified literature procedures.[29] Bis(2-amino-6-phenylphenyl) disulfide, bis(4-amino-6-phenylphenyl) disulfide and bis(2-amino-6-ethylphenyl) disulfide were prepared by the reported method.[30] (2- Or 4-R′CONH-6-$PhC_6H_3S)_2$ (R′ = Bu^t, Me or CF_3) and (2-Bu^{t}CONH-6-$EtC_6H_3S)_2$ were prepared by literature methods.[13] The complex $[NMe_4]_2[Fe_4S_4(SBu^t)_4]$·MeCN was

prepared by the literature method.[31] Four-iron ferredoxin models were synthesized by the ligand-exchange reaction of this complex with corresponding disulfides.[12]

Syntheses

$[NMe_4]_2[Fe_4S_4(SC_6H_3Ph\text{-}6\text{-}NHCOBu^t\text{-}2)_4]$ 1. The complex was synthesized by the ligand-exchange method. A mixture of $[NMe_4]_2[Fe_4S_4(SBu^t)_4]$·MeCN (49.3 mg, 0.055 mmol) and $(2\text{-}Bu^tCONH\text{-}6\text{-}PhC_6H_3S)_2$ (125 mg, 0.22 mmol) in acetonitrile (3 cm^3) was stirred at room temperature for 1 d. The solution was concentrated under reduced pressure. The black crude product was recrystallized from acetonitrile–diethyl ether and black microcrystals were obtained (43 mg, 48%) (Found: C, 55.1; H, 6.10; N, 4.85. $C_{76}H_{96}Fe_4N_6O_4S_8$ requires C, 55.75; H, 5.90; N, 5.15%).

$[NMe_4]_2[Fe_4S_4(SC_6H_3Ph\text{-}6\text{-}NHCOMe\text{-}2)_4]$ 2. The complex was synthesized by a similar method to that for **1**. A mixture of $[NMe_4]_2[Fe_4S_4(SBu^t)_4]$·MeCN (41.1 mg, 0.046 mmol) and $(2\text{-}MeCONH\text{-}6\text{-}PhC_6H_3S)_2$ (88.6 mg, 0.18 mmol) in acetonitrile (5 cm^3) was stirred at room temperature for 2 d. The solution was concentrated under reduced pressure. The black crude product was recrystallized from acetonitrile–diethyl ether to give a black oil (31 mg, 46%) (Found: C, 52.05; H, 5.25; N, 5.35. $C_{64}H_{72}Fe_4N_6O_4S_8$ requires C, 52.3; H, 4.95; N, 5.70%).

$[NMe_4]_2[Fe_4S_4(SC_6H_3Ph\text{-}6\text{-}NHCOCF_3\text{-}2)_4]$ 3. This complex was synthesized by the same method as used for **1**. The black crude product was recrystallized from acetonitrile–diethyl ether and black microcrystals were obtained. Yield 42% (Found: C, 45.6; H, 3.70; N, 4.90. $C_{64}H_{60}F_{12}Fe_4N_6O_4S_8$ requires C, 45.6; H, 3.60; N, 5.00%).

$[NMe_4]_2[Fe_4S_4(SR)_4]$ (R = $C_6H_3Ph\text{-}6\text{-}NHCOBu^t\text{-}4$ or $C_6H_3\text{-}Ph\text{-}6\text{-}NHCOCF_3\text{-}4$ 5). These complexes were synthesized by a similar method to that used for **1**. They were obtained as black oils: **4**, yield 48% (Found: C, 55.1; H, 6.10; N, 4.85. $C_{76}H_{96}Fe_4N_6O_4S_8$ requires C, 55.75; H, 5.90; N, 5.15%); **5**, yield 42% (Found: C, 45.6; H, 3.70; N, 4.90. $C_{64}H_{60}F_{12}Fe_4N_6O_4S_8$ requires C, 45.6; H, 3.60; N, 5.00%).

$[NMe_4]_2[Fe_4S_4(SC_6H_3Et\text{-}6\text{-}NHCOBu^t\text{-}2)_4]$ 6. The complex was synthesized by the ligand-exchange method. A mixture of $[NMe_4]_2[Fe_4S_4(SBu^t)_4]$ (53 mg, 0.059 mmol) and $(2\text{-}Bu^tCONH\text{-}6\text{-}EtC_6H_3S)_2$ (134 mg, 0.28 mmol) in acetonitrile (3 cm^3) was stirred at room temperature for 2 d. The solution was concentrated under reduced pressure. The black crude product was washed with ether and a black oil obtained (33 mg, 39%) (Found: C, 49.5; H, 6.65; N, 5.75. $C_{60}H_{96}Fe_4N_6O_4S_8$ requires C, 49.85; H, 6.70; N, 5.80%).

Physical measurements

The UV/VIS spectra were recorded on a Shimadzu UV-3100PC spectrophotometer in the visible region, IR spectra on a JASCO IR-8300 spectrometer as KBr pellets and ^1H NMR spectra on a JEOL JNM-EX 270 MHz Fourier-transform spectrometer with $SiMe_4$ as external reference. The T_1 values of ^1H NMR signals were obtained by the inversion-recovery method using a 180°–τ–90° pulse with a delay between 180 and 90° pulses. Cyclic voltammetry in acetonitrile solution was carried out on a BAS 100 B/W instrument with a three-electrode system: a glassy carbon working electrode, a platinum-wire auxiliary electrode and a saturated calomel electrode. The scan rate was 100 mV s^{-1}, sample concentration about 2.5 mmol dm^{-3} containing 100 mmol dm^{-3} $NBu^n_4ClO_4$ as supporting electrolyte. Potentials were determined at room temperature *vs.* the SCE as reference.

Acknowledgements

We are grateful for financial supports from the Research Fellowships of the Japan Society for the Promotion of Science for Young Scientists Fellowships (T. U., No. 2691, 1995–1998) for Japanese Junior Scientists and for a Grant-in-Aid for Specially Promoted Research from the Ministry of Education, Science and Culture (A. N., No. 06101004).

References

1 D. R. Breiter, T. E. Meyer, I. Rayment and H. M. Holden, *J. Biol. Chem.*, 1991, **266**, 18660.
2 I. Rayment, G. Wesenberg, T. E. Meyer, M. A. Cusanovich and H. M. Holden, *J. Mol. Biol.*, 1992, **228**, 672.
3 C. W. Carter, jun., in *Iron–Sulphur Proteins*, ed. W. Lovenberg, Academic Press, New York, 1977, vol. III, p. 158.
4 N. Ueyama, T. Terakawa, T. Sugawara, M. Fuji and A. Nakamura, *Chem. Lett.*, 1984, 1287.
5 Y. Okuno, K. Uoto, O. Yonemitsu and T. Tomohiro, *J. Chem. Soc., Chem. Commun.*, 1987, 1018.
6 M. Nakamoto, K. Tanaka and T. Tanaka, *Bull. Chem. Soc. Jpn.*, 1988, **61**, 4099.
7 T. E. Meyer, C. T. Przysiecki, J. A. Watkins, A. Bhattacharyya, R. P. Simondsen, M. A. Cusanovich and G. Tollin, *Proc. Natl. Acad. Sci. USA*, 1983, **80**, 6740.
8 R. Krishnamoorthi, J. L. Markley, M. A. Cusanovich, C. T. Przysiecki and T. E. Meyer, *Biochemistry*, 1986, **25**, 60.
9 S. M. Lui and J. A. Cowan, *J. Am. Chem. Soc.*, 1994, **116**, 4483.
10 N. Ueyama, T. Terakawa, M. Nakata and A. Nakamura, *J. Am. Chem. Soc.*, 1983, **105**, 7098.
11 R. Ohno, N. Ueyama and A. Nakamura, *Inorg. Chem.*, 1991, **30**, 4887.
12 N. Ueyama, Y. Yamada, T. Okamura, S. Kimura and A. Nakamura, unpublished work.
13 N. Ueyama, T. Okamura and A. Nakamura, *J. Am. Chem. Soc.*, 1992, **114**, 8129.
14 N. Ueyama, T. Okamura, Y. Yamada and A. Nakamura, *J. Org. Chem.*, 1995, **60**, 4893.
15 T. Okamura, N. Ueyama, A. Nakamura, E. W. Ainscough, A. M. Brodie and J. M. Waters, *J. Chem. Soc., Chem. Commun.*, 1993, 1658.
16 L. Banci, I. Bertini, A. Dikiy, D. H. W. Kastrau, C. Luchinat and P. Sompornpisut, *Biochemistry*, 1995, **34**, 206.
17 H. Rüterjans, L. Messori, O. Ohlenschläger, F. Briganti and I. Bertini, *Appl. Magn. Reson.*, 1993, **4**, 477.
18 R. H. Holm, W. D. Phillips, B. A. Averill, J. J. Mayerle and T. Herskovitz, *J. Am. Chem. Soc.*, 1974, **96**, 2109.
19 N. Ueyama and A. Nakamura, in *Metalloproteins*, eds. S. Otsuka and T. Yamanaka, Elsevier, Amsterdam, 1988, p. 153.
20 J. G. Reynolds, E. J. Laskowski and R. H. Holm, *J. Am. Chem. Soc.*, 1978, **100**, 5315.
21 A. Aizman and D. A. Case, *J. Am. Chem. Soc.*, 1982, **104**, 3269.
22 B. V. DePamphilis, B. A. Averill, T. Herskovitz, J. L. Que and R. H. Holm, *J. Am. Chem. Soc.*, 1974, **96**, 4159.
23 J. Zhou, M. J. Scott, Z. Hu, G. Peng, E. Münck and R. H. Holm, *J. Am. Chem. Soc.*, 1992, **114**, 10843.
24 C. W. Carter, *J. Biol. Chem.*, 1977, **252**, 7802.
25 N. Ueyama, T. Sugawara, M. Fuji, A. Nakamura and N. Yasuoka, *Chem. Lett.*, 1985, 175.
26 P. K. Mascharak, K. S. Hagen, J. T. Spence and R. H. Holm, *Inorg. Chim. Acta*, 1983, **80**, 157.
27 B. Liedholm, *Acta Chem. Scand., Ser. B*, 1976, **30**, 141.
28 S. Sako, *Bull. Chem. Soc. Jpn.*, 1934, **9**, 55.
29 T. Wagner-Jauregg and E. Helmert, *Chem. Ber.*, 1942, **75**, 935.
30 S. Keimatsu and I. Satoda, *J. Pharm. Soc. Jpn.*, 1936, **56**, 600.
31 B. A. Averill, T. Herskovitz, R. H. Holm and J. A. Ibers, *J. Am. Chem. Soc.*, 1973, **95**, 3523.

Received 2nd *February* 1996; *Paper* 6/00785F